

# The replacement and refurbishment of Gap Scintillator Counters for the ATLAS Tile Calorimeter Phase I Upgrade

G Mokgatitswane<sup>1</sup>, T J Lepota<sup>1</sup> and B Mellado<sup>1,2</sup>

<sup>1</sup> School of Physics and Institute for Collider Particle Physics, University of the Witwatersrand, Johannesburg, Wits 2050, South Africa

<sup>2</sup> iThemba LABS, North, Empire Road, Braamfontein 2000, Johannesburg

E-mail: gaogalalwe.mokgatitswane@cern.ch

**Abstract.** We report on the replacement of E3 and E4 scintillators (Crack) and refurbishment of Minimum Bias Trigger Scintillator (MBTS) counters as part of Phase I upgrade of the Tile Calorimeter of the ATLAS experiment during the long shutdown 2. The Crack and MBTS counters, situated between the central and extended Tile Calorimeter barrels, are used for correcting the electromagnetic energy responses and for providing inputs to the trigger, respectively. During the LHC Run 2 data-taking period in 2015-2018, the Crack and MBTS scintillators have deteriorated by radiation and had to be replaced with more radiation-hard scintillators and optimised geometry for Run 3. The Phase I upgrade has been ongoing since the beginning of the LHC LS2. The upgrade activities which were finalized with a strong contribution from South Africa consisted of the re-design of the Crack and MBTS detector modules, their assembly, qualification and characterization using radioactive sources (strontium-90 and cesium-137), as well as their installation on the ATLAS detector. The University of the Witwatersrand was previously involved in the radiation qualification and selection of the scintillator material to be used in the counter production.

## 1. Introduction

During Phase I upgrade of the ATLAS Experiment, the Tile Calorimeter (TileCal) completely replaced the Crack and MBTS scintillators since they were degraded by high levels of radiation (up to  $10^3$  Gy/year) during the LHC Run 2 data-taking period spanning 2015-2018 [1]. Prior to the first run of the LHC at centre-of-mass energy of 7 TeV of proton-proton ( $pp$ ) head-on collision (Run 1), radiation background simulations were conducted to identify and quantify the detrimental effects of these backgrounds on the performance of detector components. The general-purpose Monte Carlo particle transport programs FLUKA [2] and GEANT3-CALOR (GCALOR) [3] were used to predict the background radiation in ATLAS. It was predicted that the sub-detector components in close proximity to the beam axis would receive higher radiation dose rates.

The MBTS counters were originally intended to operate only in the early running of the LHC, where the vast majority of crossings would not result in large pile-up. Thus, the counters would serve to provide a trigger to discriminate beam-beam interactions from beam-gas interactions. Originally, there were no TileCal electronic channels available for the MBTS counter



**Figure 1.** A photograph of one of the MBTS counters after irradiation (Run 2).

readout. To create the needed channels, one-eighth of the Crack counters were removed from the detector, and the light signals from the MBTS counters were connected to the optical cables originally used for the missing Crack counters. Later, for Run 2, additional channels were made available by the merging of the light signals from adjacent E1 counters, and the missing Crack scintillators were replaced.

Figure 1 shows one sector of the MBTS counter, where intense radiation damage is indicated by the yellowing of the scintillator (loss of up to 95% of the light yield). The radiation dose at the inner radius was of the order of 20 MRad. The Crack counters are located at a lower rapidity, but in the case of E4, in a region corresponding to electromagnetic shower max. This position results in a higher radiation dose, but an accurate sampling of the energy deposited by electrons and photons in this region is crucial for improving the energy resolution degraded by the material present.

## **2. Crack and MBTS geometry optimisation and scintillating materials used in counter production**

### *2.1. Crack counters*

The Crack counters were extended from a maximum pseudo-rapidity coverage from up to 1.6 to up to 1.72 (see Figure 2), motivated by the need to improve the  $e/\gamma$  energy resolution in this extended range. This is supported by multivariate analysis (MVA) calibration of the reconstructed electron energy in the extended range [4], which shows a significant improvement in the energy resolution (see Figure 3). Based on simulation and rate studies, the decision was made to have the E3 section cover the rapidity range from 1.2 to 1.6, and to then use the freed-up E4 channels to cover the region from 1.6 to 1.72. The rate in the old E3 counter (1.2–1.4) was significantly smaller than in the old E4 counter (1.4–1.6), so combining the two rapidity regions in the same readout did not seriously affect the performance. This results in reasonable rates for both the new E3 and E4 counters.

A new Crack counter is composed of a radiation hard and high-performing PolyvinylToluene (PVT) based plastic scintillator (EJ-208). It has a long emission spectrum (435 nm) which provides additional resistance to radiation damage. The wavelength shifting (WLS) Y-11 optical fibers (high light yield) are used to collect light emitted by the scintillating tiles (blue to green shifters), which is then transported by clear optical fiber cable to the photomultiplier tubes in

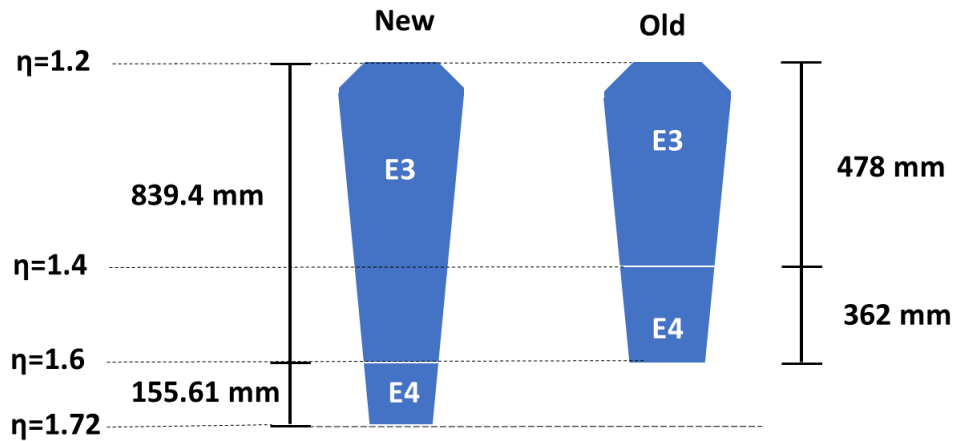


**Figure 2.** Sketch of the geometry of old Crack scintillation counter vs. the geometry of the new counters.

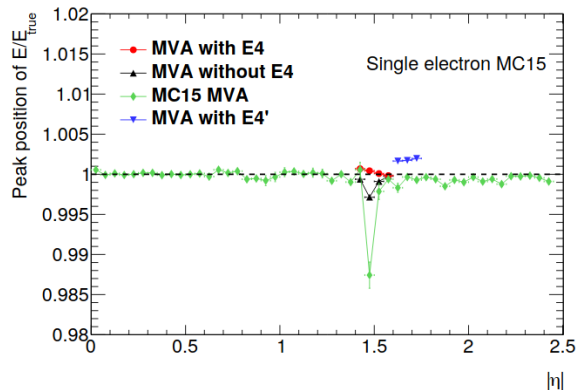


**Figure 3.** Resolution as a function of pseudorapidity for electrons [4].

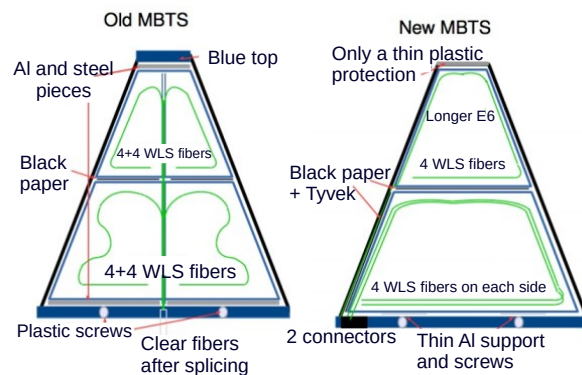


**Figure 4.** MBTS geometry optimisation.

the TileCal girder.

### 2.2. Minimum Bias Trigger Scintillators (MBTS)

During the studies of potential radiation hard plastic scintillator, it was found that commercially available plastic scintillators would still succumb to high doses in the MBTS region and hence degrade. In order to counterbalance the degradation effect, several optimisations were proposed. The first optimisation was the replacement of one 20 mm thick scintillator plate with a sandwich of four 5 mm scintillators, each wrapped individually with Tyvek (a material made of 100% high-density polyethylene, acting as a diffuser).

One reason for using thin plates was to allow for oxygen diffusion into the scintillators, which plays a vital role in annealing of radiation induced optical color centers. This phenomenon improves light transmission and therefore helps in recovery of scintillator slabs after exposure to high energy particles. The second optimisation was the placement of the WLS fibres in the grooves on both sides of the large (outer) plates, to improve the light collection properties, as opposed to several fibres in the same groove on one side [5] (see Figure 4)



**Figure 5.** Assembly of a Crack counter.

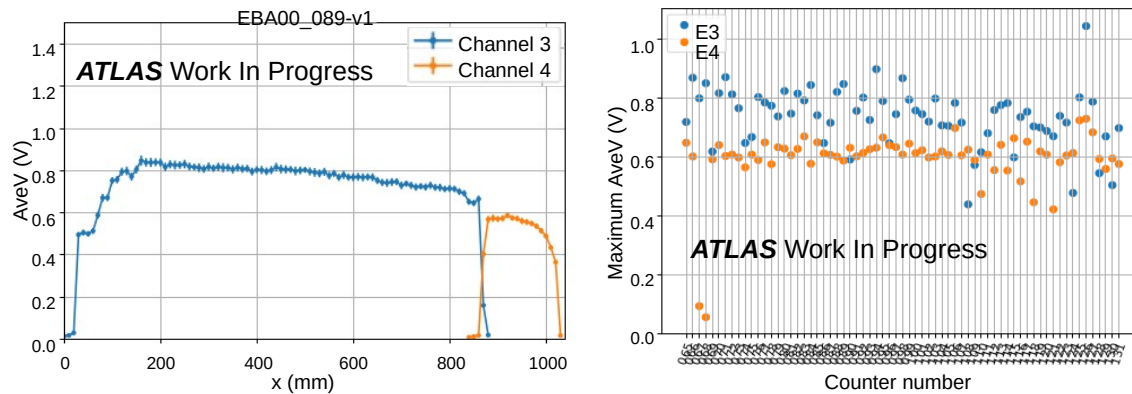


**Figure 6.** Fine scan (10 mm step) of EBA-089 counter (left) and the highest signal output for all EBA counters (right).

### 3. Assembly of Crack and MBTS counters

A Tyvek was used to wrap each scintillator slab [5], together with their corresponding coupled WLS optical fibers. Tyvek is specially designed to trap the scintillation light through internal reflection and also provides mechanical protection. The wrapped slabs were then placed inside the aluminium cover constructed to house the scintillator slabs, providing mechanical protection as well as eliminating the possibilities of light leakage. Figure 5 is shown a Crack counter being assembled. A standard assembly procedure was followed for both counters.

### 4. Qualification and characterization of assembled counters

Prior to installation of the assembled counters on the ATLAS detector, their quality had to be assured. The certification and characterization was performed using  $^{90}\text{Sr}$  and  $^{137}\text{Cs}$  radioactive sources located at CERN B175 laboratory [6].

#### 4.1. $^{90}\text{Sr}$ tests

The E3 and E4 segments of the counter were tested using  $^{90}\text{Sr}$  scans. The experimental setup comprised of a light-tight scan box containing a photomultiplier tube (PMT), a high voltage source to supply the PMT with 700 V, clear optical fiber cable (6 fibers) to connect the counter to the PMT, a digital multimeter for readout,  $^{90}\text{Sr}$   $\beta$ -electron source of 25 MBq activity and recording system to record the data [6].

The E3 and E4 segments of the counter were both evaluated to check for any possible light leaks. Prior to performing  $^{90}\text{Sr}$  scans, the pedestal was measured where the signal across the PMT was read without  $^{90}\text{Sr}$  source on the counter segments. After measuring the pedestal, the source was then introduced and moved along the  $x$ -axis of the counter while taking the reading in each step. Figure 6 shows a plot of PMT average voltage (aveV) response versus source position ( $x$ ) on the scintillator and the maximum aveV output for all EBA counters (right).

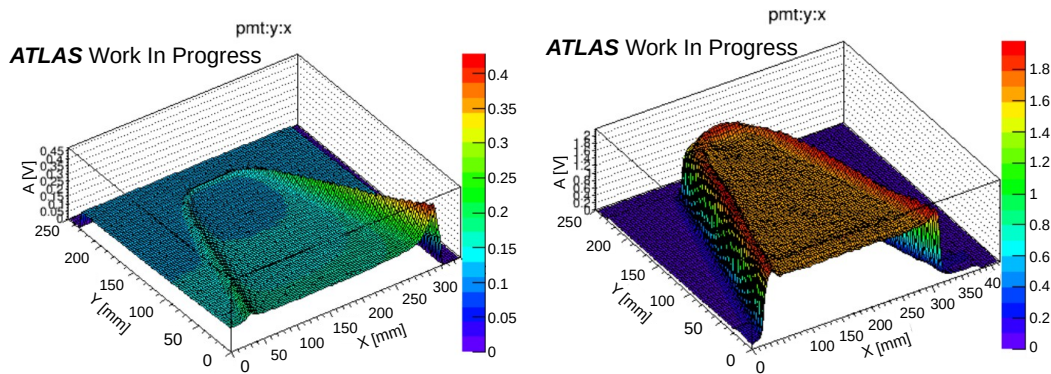


**Figure 7.**  $^{90}\text{Sr}$  2D scans of the old inner MBTS UPS923A with 4x old WLS Y-11 fibres (left) and new inner MBTS EJ200 with 1x new WLS Y-11 (right).

The low response of E4 segments for counters 67 and 68 (special counters) is because of using orange fibers for readout. Orange fibers attenuate more light due to short light attenuation length ( $> 1.5$  m) in comparison with green fibers ( $> 3.5$  m), hence the response was expected. The performance of orange fibers would be studied during Run 3 and compared with green fibers.

#### 4.2. $^{90}\text{Sr}$ scanning of new and old inner MBTS scintillators

The assessment of the performance of old and new inner MBTS scintillators from the C-Side of ATLAS was conducted by testing their response to a  $^{90}\text{Sr}$   $\beta$ -electron source. The signal generated by the PMT was measured as a function of radiation source position and a 2D scan of signal was measured in the  $x$  and  $y$  direction over the inner MBTS scintillator. Figure 7 shows 2D scans of a 20 mm thick old inner MBTS UPS923A with 4x old WLS Y-11 green fibres (left) and a new inner MBTS EJ200 scintillator with 1x new WLS Y-11 green fibre (right). According to the results, response of the old scintillator to  $^{90}\text{Sr}$  was low in comparison with the new EJ200 scintillator, which was attributed to degradation undergone by the old scintillators during Run 2. However, the old WLS Y-11 fibres appeared to be less damaged since their response was comparable to that of new fibres.

#### 4.3. $^{137}\text{Cs}$ tests

The MBTS counters were evaluated using the  $^{137}\text{Cs}$  system from a spare extended barrel (EB) module. The  $^{137}\text{Cs}$   $\gamma$  source of 250 MBq activity embedded in the metal capsule is transported by liquid flow inside the tubes passing towards the MBTS counter [7]. The counter was attached to the edge of EB module, where the tubes are going out of the calorimeter module.

When a source approaches the counter, photons with the energy  $E_\gamma=0.662$  MeV excite light emission in the scintillating slabs and that allows a measurement of the optical quality of the slabs and fibres. The inner (E6) and outer (E5) counters were each connected to PMT2 and PMT14, respectively, using a clear optical fibre cable (3 m). Figure 8 show plots of ADC counts versus trigger (after subtracting the pedestal) as the source travels towards the MBTS counter (left) and a zoomed peak showing the maximum ADC count value for the inner counter (right).

The maximum ADC counts for inner and outer counters were calculated by taking the integral of the peaks. The limits for integration on the  $x$ -axis (trigger) were defined by fixing the threshold at 50 ADC counts. Since the speed of  $^{137}\text{Cs}$  source travelling through the tube would differ from run to run, the maximum ADC integral value obtained was divided by width of the peak to get an average value. Figure 9 shows the relative maximum ADC integral and average values versus  $\phi$  position of the MBTS detector modules for side C of ATLAS.

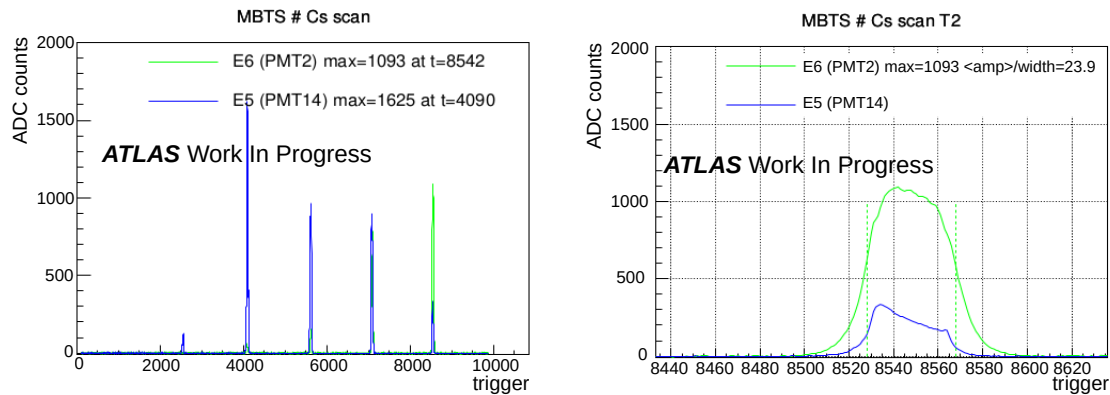


**Figure 8.** Signal response of the inner and outer MBTS counters to  $^{137}\text{Cs}$  source.

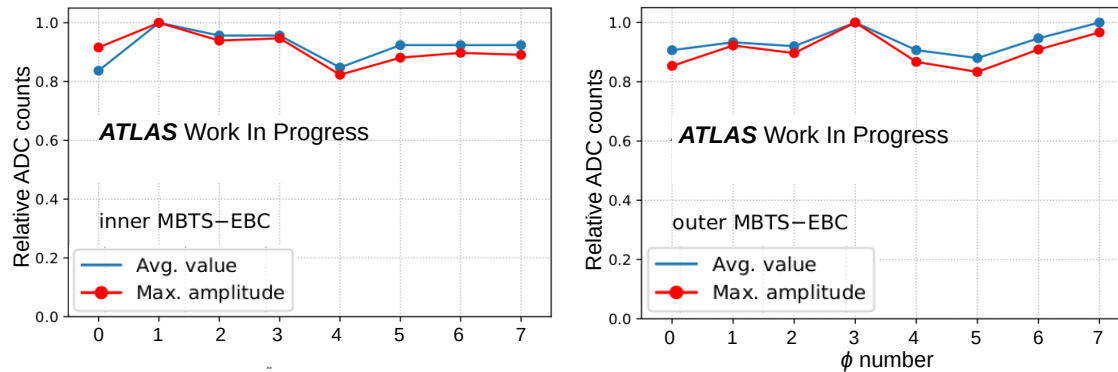


**Figure 9.** Relative ADC counts of maximum amplitude and average for side-C inner counters (left) and outer counters(right).

## 5. Conclusion

The Phase I upgrade at CERN commenced since the beginning of LHC long shutdown 2 where the TileCal was completely replacing and refurbishing the E3 and E4 and MBTS counters. These counters were degraded by high radiation levels during the LHC Run 2 and had to be replaced with high-performing and more radiation hard scintillator prior to Run 3. Both counters have undergone several improvements with respect to LHC Run 1 and Run 2 to maximise the light yield and their performance efficiency. Phase I upgrade was completed with a strong contribution from South Africa.

## References

- [1] Aad G *et al.* (ATLAS) 2011 Letter of Intent for the Phase-I Upgrade of the ATLAS Experiment Tech. rep. CERN Geneva (CERN-LHCC-2011-012)
- [2] Ferrari A, Sala P R, Fassò A and Ranft J 2005 *FLUKA: A multi-particle transport code (program version 2005)* CERN Yellow Reports: Monographs (Geneva: CERN)
- [3] Zeitnitz C and Gabriel T 1994 *Nucl. Instrum. Meth. A* **349** 106–111
- [4] Durglishvili A 2020 Ph.D. thesis CERN (CERN-THESIS-2020-110)
- [5] Scheu S, Kaspar H, Robmann P, van der Schaaf A and Truol P 2006 *Nucl. Instrum. Meth. A* **567** 345–349
- [6] Baranov V *et al.* 2018 *Nucl. Instrum. Methods Phys. Res. B* **436** 236–243
- [7] Blanchot G *et al.* 2020 *J. Instrum.* **15** 03017